Pakistan J. Zool., vol. 54(4), pp 1791-1802, 2022 DOI: https://dx.doi.org/10.17582/journal.pjz/20210129120146

Effects of *Moringa oleifera*, Curcumin, and Green Tea Extracts on Histopathological Changes in Mesenteric Lymph Nodes and Spleen of Albino Rats with Benzene-Induced Leukemia

Ahmed Alazzouni[1], Ashraf Al-Brakati[2,*], Sherif Rabie[1], Mohamed Gabry[1] and Basmaa Hassan[1]

[1]*Department of Zoology and Entomology, Faculty of Science, Helwan University, Helwan, Cairo Governorate 11111, Egypt*
[2] *Department of Human Anatomy, College of Medicine, Taif University, P.O. Box 11099, Taif 21944, Saudi Arabia*

ABSTRACT

This study evaluated the protective effect of *Moringa oleifera*, curcumin, and green tea extracts against benzene chromasolv-induced leukaemia in rats and their ability to alleviate the histopathological alterations in the mesenteric lymph nodes (MLNs) and spleen. In this study 70 rats were divided into seven groups as follow: control, benzene (0.2 ml twice/week), *Moringa oleifera* (100 mg/kg), curcumin (300 mg/kg), green tea (350 mg/kg), combined green tea and curcumin, and cyclophosphamide (7.5 mg/kg) groups. All groups were treated for one month after the induction of leukemia. We found that the extracts ameliorated most histopathological changes in MLNs and spleens in rats exposed to benzene, restoring normal mast cell counts and elastic fiber area percent in a benzene-induced leukaemia model. To conclude *Moringa oleifera*, curcumin, and green tea extracts could be used as natural chemotherapeutic agents and as adjuvants to ameliorate histopathological changes associated with leukemia.

Article Information
Received 29 January 2021
Revised 23 March 2021
Accepted 18 April 2021
Available online 12 August 2021 (early access)
Published 22 April 2022

Authors' Contribution
AAB and BH conceived the project. AAB prepared first draft of the article. AA performed the experiments. SR and BH helped in experimental work. BH provided resources and supervised the work.

Key words
Leukemia, *Moringa oleifera*, Curcumin, Green tea, Lymph nodes.

INTRODUCTION

The global prevalence of leukemia is reported to be 5.8 and 4.3 per 100,000 person-years in men and women, respectively (Ahmadi *et al*., 2016). Leukemia refers to cancers that begin in blood-forming cells of the body; these abnormal cells grow and multiply in an uncontrolled manner (Roy *et al*., 2014). Leukemia is rooted in the Latin language and means "white blood"; it disrupts the body's natural immunity and erythropoiesis. Leukemia induces the accumulation of cells outside the bone marrow, forming masses in vital organs of the body, such as the brain, lymph node (LN), spleen, and liver (Varkesh *et al*., 2013). Chronic exposure to benzene is associated with a variety of hematological disorders, such as aplastic anemia, myeloproliferative disorders, and most detrimentally, leukemia, with acute myeloid leukemia (AML) the most common (Khalade *et al*., 2010). Cyclophosphamide (CP) is a synthetic alkylating agent chemically related to the nitrogen mustards (Netíková *et al*., 2018). It is effective against a wide spectrum of malignancies, such as leukemia, lymphoma, breast, lung, prostate, and ovarian cancers (Chen *et al*., 2018). The side effects of cytotoxic drugs are major obstacles for treatment success (Fares, 2015).

Many substances derived from dietary or medicinal plants are known to be effective and versatile chemopreventive and antitumor agents in a number of experimental models of carcinogenesis (Abdellatef *et al*., 2010). Cancer therapeutic agents block mechanisms involved in inducing cancer processes (Ke and Shen, 2017). *Moringa oleifera* (Family: Moringaceae) is a multipurpose tree that is used as a vegetable, spice, a source of cooking and cosmetic oil, and a medicinal plant (Abdellatef *et al*., 2010). Leaves of *Moringa oleifera* are rich in compounds with anticancer activity, including 4(4'-O-acetyl-L-rhamnopyranosyloxy) benzyl isothiocyanate, and 4-(-L-rhamnopyranosyloxy) benzyl glucosinolate (Abdellatef *et al*., 2010). The active constituents of turmeric are the flavonoid curcumin (diferuloylmethane) and various volatile oils (Verma *et al*., 2018). Curcumin is one of the most promising chemopreventive agents against a variety of human cancers, including colon, duodenal, stomach, prostate, leukemia, and breast cancers

* Corresponding author: a.albrakati@tu.edu.sa
0030-9923/2022/0004-1791 $ 9.00/0

(Sinha *et al*., 2012). The most active constituents of green tea are polyphenols (catechins) (Musial *et al*., 2020). Green tea contains high quantities of several polyphenolic components, which have antioxidant and antimutagenic effects (Maiti *et al*., 2019). Epigallocatechin-3-gallate (EGCG) is the predominant polyphenol in catechin green tea extract (GTE) and plays a central role in the anticancer effects of green tea polyphenols. Recent studies have demonstrated that EGCG has anticancer effects in hematopoietic malignancy (Kumazoe *et al*., 2015).

The present study was designed to demonstrate the anti-leukemic role of *Moringa oleifera*, curcumin and green tea in a benzene-induced leukemia model in albino rats through assessment of hematological parameters. Additionally, this study evaluated the ameliorative role of these herbal products in histopathological alterations in the spleen and LNs of leukemic rats.

MATERIALS AND METHODS

Chemicals and extracts

Moringa oleifera leaf aqueous extract was obtained from the National Research Center (NRC), Dukki, Egypt. Curcumin was obtained as turmeric extract, standardized to contain 95% curcuminoids with high antioxidant power in 500 mg capsules, and manufactured by Puritan's pride, Inc., U.S.A. Green tea extract (GTE) tablets were obtained as super antioxidant green tea leaf, standardized to contain 500 mg GTE, yielding 175 mg EGCG, and manufactured by Source Naturals, Inc., U.S.A. Benzene Chromasolv was obtained as benzene with a purity > 99.9%, was used in chromatographic analysis, and purchased from Sigma-Aldrich Corp., St Louis, USA. CP (Endoxan) was obtained as 200 mg powder manufactured by Baxter Oncology (Germany, Alemania), and imported by Egydrug. Other chemicals and dyes were of analytical grade and were purchased from El-Gomhouria Co. (Cairo, Egypt).

Experimental design

A total of 70 female albino rats (*Rattus norvegicus*) weighing 200 ± 20 kg were purchased from the New Veterinary Office (Cairo, Egypt). Rats were housed in wired cages in a temperature-controlled environment with 12-h light/dark cycles. Food and water were freely available throughout the experiment. Rats were divided into the following groups (10 rats per group): Group 1 (control group) received only distilled water through the experimental period; Group 2 (benzene group, leukemia positive control) received 0.2 mL benzene solution (twice/week) intravenously in the tail vein for 3 months according to Akanni *et al*. (2014); Group 3 (*Moringa oleifera* treated group) received 100 mg/kg/day *Moringa oleifera* extract by gastric tube for 1 month after leukemia induction, according to the dose used by Akanni *et al*. (2014); Group 4 (curcumin treated group) received 300 mg/kg/day orally for 1 month after leukemia induction, according to Tomita *et al*. (2006); Group 5 (GTE treated group) received 350 mg/kg/day GTE orally for 1 month after leukemia induction (Laurence and Bacharach, 2013); Group 6 (combined GTE + curcumin treated group) received 350 mg/kg/day GTE, and then given 300 mg/kg/day curcumin in a sequential fashion by gastric tube for 1 month according to Ghosh *et al*. (2009). Group 7 (CP treated leukemic group) received 7.5 mg/kg CP intraperitoneally every 48 h for 1 month after leukemia induction (Akanni *et al*., 2014).

Hematological assay

Leukemia induction was evaluated based on hematological parameters in the benzene-injected group compared to the control group. Blood was analyzed using a hematology analyzer for total white blood cells (WBCs), total red blood cells (RBCS), hemoglobin (Hb) concentration, packed cell volume (PCV), and Figurelet count.

Histological assay

Paraffin sections were observed for spleen and mesenteric lymph nodes (MLNs) and stained by routine hematoxylin and eosin staining (Culling and Albert, 2013). Mast cells within MLNs were stained by toluidine blue for mast cell count detection. Mast cells were counted from five different micrographs/group and the average mast cell value was used for each group. MLNs and spleen elastic fibers were stained with Orcein for morphometric analysis of elastic fibers area percent in the study groups. Five different micrographs/group were calculated using ImageJ version 1.50i, based on the masking of elastic fibers.

Statistical analysis

All numerical data were statistically analyzed and expressed as the mean ± standard deviation (SD). The level of statistical significance was set at $p < 0.05$, using a one-way analysis of variance test. Further comparisons among groups were conducted according to Tukey's post hoc test using the Statistical Package for the Social Sciences (SPSS) version 20.

RESULTS

Hematological parameters

In the present study, the complete blood count showed a significant increase in WBC counts (marked leukocytosis), and decrease in RBC counts, Hb, PCV, and Figurelet counts in the benzene-treated group when compared to the control group. These data suggested the successful induction of leukemia by intravenous injection of benzene Chromasolv (0.2 mL twice per week) in albino

rats. In rats receiving 100 mg/kg/day *Moringa oleifera*, 300 mg/kg/day curcumin, 350 mg/kg GTE, combined curcumin and GTE, and 7.5 mg/kg/48 h CP, WBC counts decreased, while RBC counts, Hb, hematocrit, and Figurelet count increased (Table I). The data shows amelioration of blood parameters in all treatment groups, which suggests the potential role of these natural products as anti-leukemic agents, similar to anti-leukemic drugs (CP).

Table I.- Hematological parameters in the various experimental rat groups expressed as mean ± SD.

Group	Control (n=10)	Benzene treated (n=10)	MO treated (n=10)	Curcumin treated (n=10)	GTE treated (n=10)	GTE+ curcumin treated (n=10)	CP treated (n=10)
WBCs	9.90±1.67	23.40±0.96*	10.70±0.27	11.26±0.53	12.28±0.65	10.08±0.80	8.90±1.21
RBCs	5.16±0.42	2.84±0.21*	4.84±0.11	4.74±0.23	4.62±0.36	4.82±0.36	5.12±0.57
Hb	13.76±0.59	7.75±0.68*	13.42±0.53	13.14±1.07	13.00±0.82	13.40±0.65	13.78±0.46
HCT	44.32±2.11	27.36±1.31*	42.18±0.87	41.82±1.73	40.76±1.67	42.84±1.33	43.12±1.43
PLT	475.0±142	233.3±25.1*	478.3±7.6	486.6±12.5	482.3±29.2	486.67±35.1	476.67±23

MO, *Moringa oleifera;* GTE, green tea extract; CP, cyclophosphamide; WBCs, white blood cell ($x10^3$cell/mm^3); RBCs, red blood corpuscles ($x10^6$cell/mm^3); Hb, hemoglobin concentration (gram/deciliter); HCT, hematocrit (%); PLT, platelets ($x10^3$cell/mm^3). *: significant difference at $p \leq 0.05$.

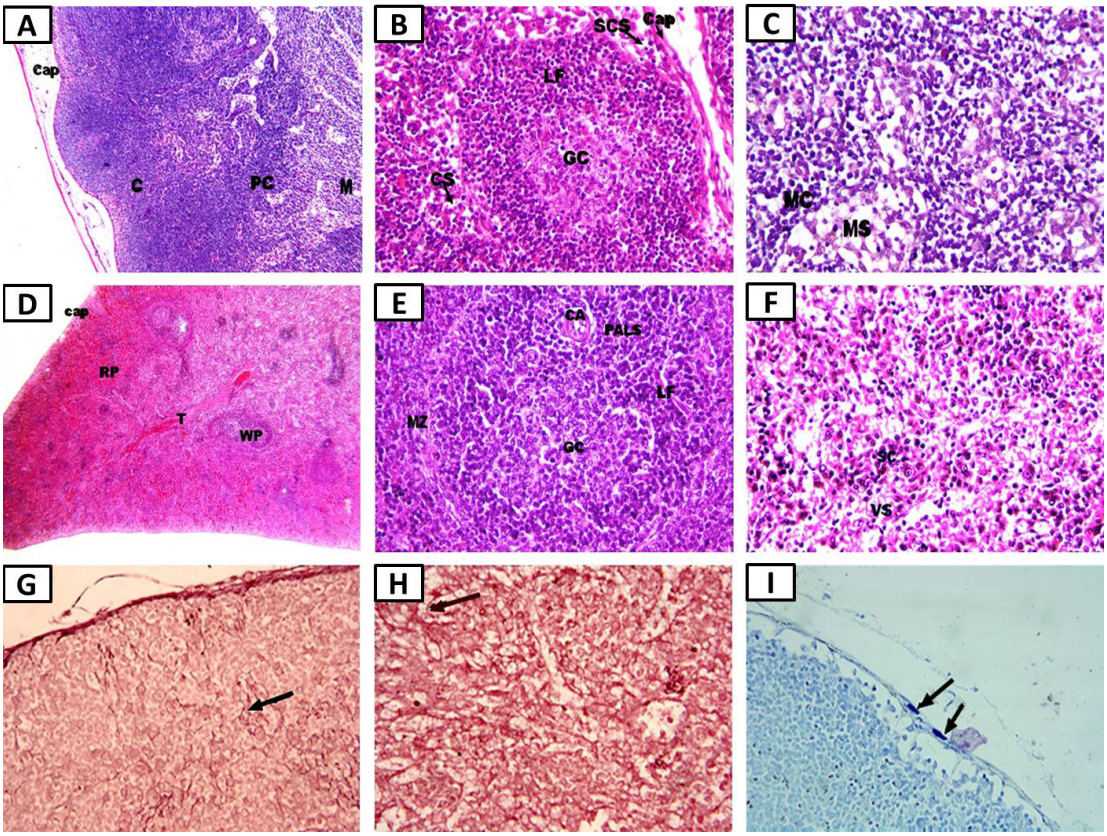

Fig. 1. Photomicrographs of the negative control group showing: A, normal mesenteric lymph node structure with cortex (C), paracortex (PC), and medulla (M) (×100); B, cortex with lymphoid follicle (LF), germinal center (GC), capsule (Cap), cortical sinuses (CS), and subcapsular sinus (SCS) (×400); C, medulla with medullary cords (MC) and medullary sinuses (MS) (×400); D, normal spleen structure with white pulp (WP) or lymphoid follicles (LF), vascular red pulp (RP), outer capsule (C), and trabeculae (T) (×100); E, white pulp's LFs with germinal center (GC), periarteriolar lymphatic sheath (PALS), central arteriole (CA), and marginal zone (MZ) (×400); F, red pulp (RP) with splenic cords (SC) and venous sinuses (VS) (hematoxylin and eosin, ×400); G, normal thin delicate elastic fibers in lymph node cortex (arrow) (×400); H, normal thin delicate elastic fibers in spleen RP (arrow) (Orcein, ×400); I, normal number of flattened mast cells (arrows) in the pericapsular connective tissue of the lymph node (toluidine blue, ×400).

Histological parameters

Figure 1A shows the normal structure of the MLNs where cortex (C) (B cell zone), para cortex (PC) (T cell zone), and medulla (M). The cortex consists of lymphoid follicles (LF) and germinal centers (GC) with lymphatic follicles (LF) that contain germinal centers (GC) (Fig. 1B). Medulla consists of medullary cords (MC) and medullary sinuses (MS) (Fig. 1C). The histological architecture of the control spleen (Fig. 1D); consists of white pulp (WP) and red pulp (RP). WP mainly exists in LF with a central arteriole (CA) and a periarteriolar lymphatic sheath (PALS), GC, and marginal zone (MZ) (Fig. 1E). RP consists of splenic cords (SC) and venous sinuses (VS) in between (Fig. 1F). Figure 1G showed thin, delicate elastic fibers dispersed in MLNs and thin, delicate elastic fibers dispersed in the spleen (Fig. 1H). There are few normal mast cells in the pericapsular area surrounding MLN (Fig. 1I).

The benzene-injected group showed abnormal LN structure (Fig. 2A), cortical changes with necrotic (ghost) cells, and dilated and congested cortical sinus (CS) (Fig. 2B), LN medullary changes with dilated and congested high endothelial venules (HEVs) (Fig. 2C), dilated spleen congested pulp arteries (PA) (Fig. 2D),

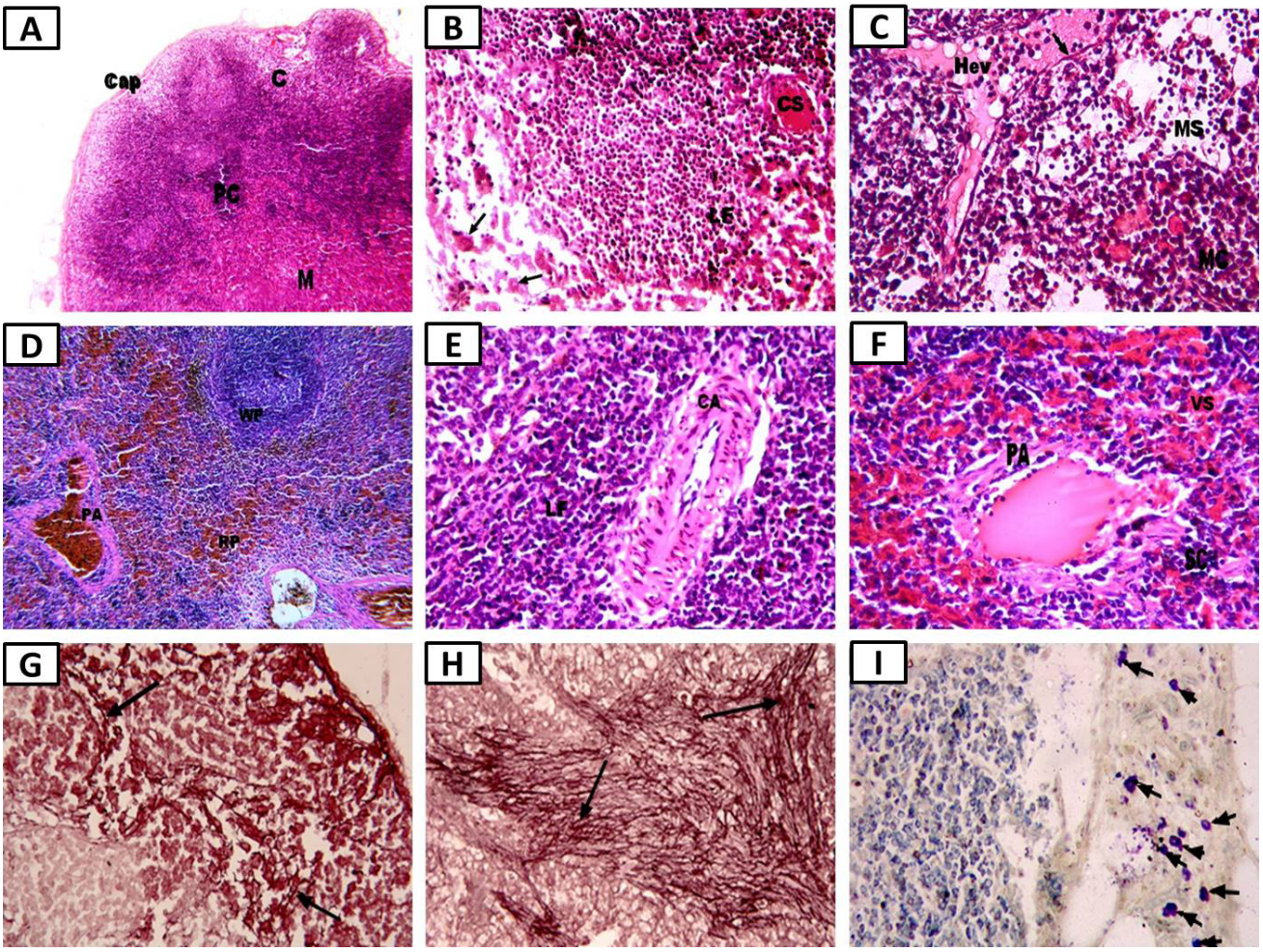

Fig. 2. Photomicrographs of the benzene-injected group showing: A, whole lymph node structure (×100); B, cortical changes with some necrotic (ghost) cells (arrow), dilated, congested cortical sinus (CS), and non-active lymphoid follicles (LF) (×400); C, medullary changes with dilated and congested high endothelial venules (HEVs) lined with simple squamous epithelium (arrow) (×400); D, spleen with dilated congested pulp artery (PA) (×100); E, white pulp (WP) with thick dilated central arteriole (CA) in non-active LF (×400); F, red pulp (RP) with congested venous sinuses (VS) and dilated PA (hematoxylin and eosin, ×400); G, densely stained irregular thick elastic fibers (arrow) (×400); H, thick elastic fiber aggregation in the spleen (arrow) (Orcein, ×400); I, increased numbers and larger than normal mast cells (arrows) in the pericapsular connective tissue of the lymph node (toluidine blue, ×400).

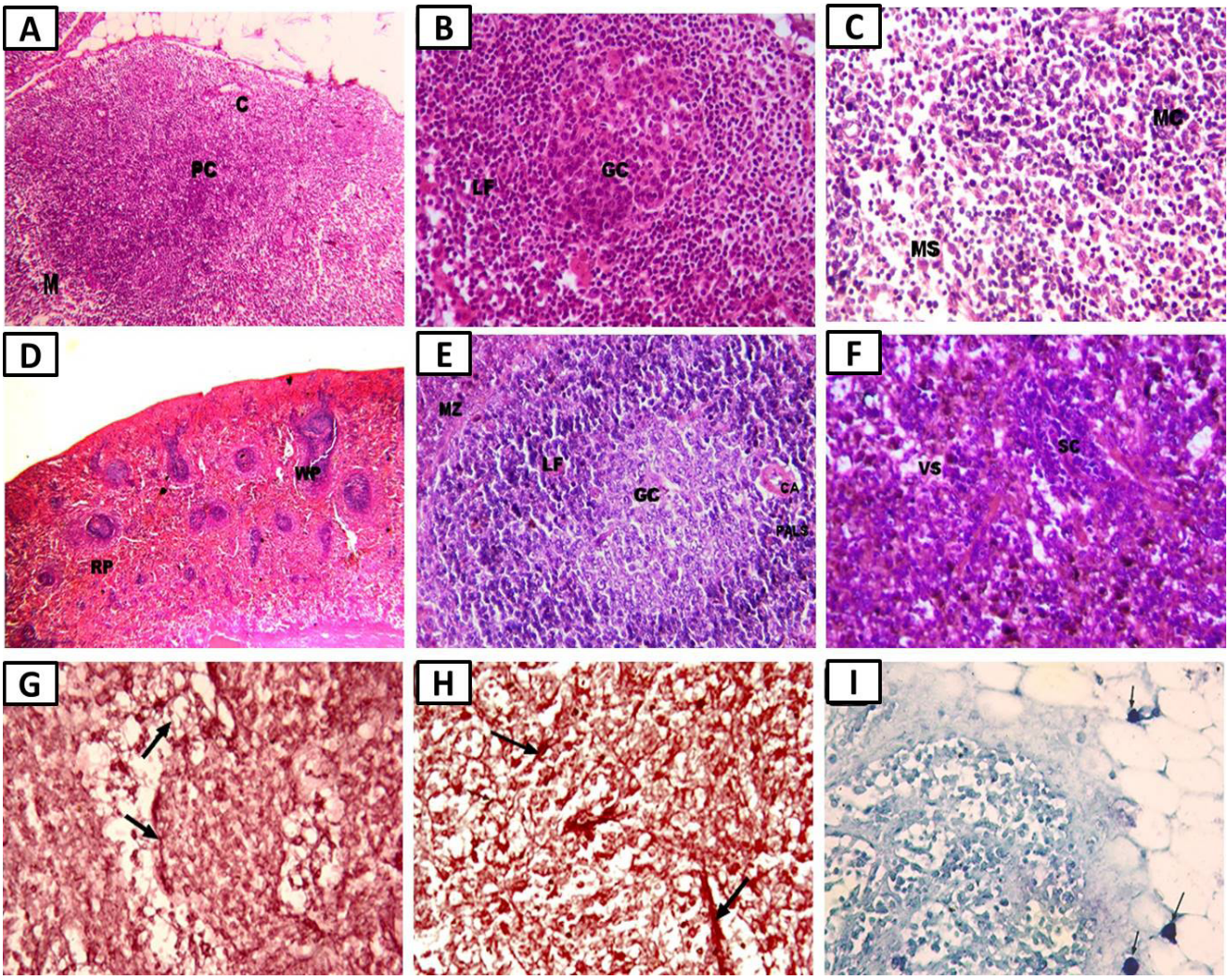

Fig. 3. Photomicrographs of the *M. oleifera* treatment group showing: A, marked improvement in lymph node structure with cortex (C), paracortex (PC), and medulla (M) (×100); B, cortical lymphoid follicle (LF) with germinal center (GC) (×400); C, medulla with medullary cords (MC) and medullary sinuses (MS) (×400); D, marked improvement in spleen white pulp (WP) and red pulp (RP) structure (×100); E, WP with LF, central arteriole (CA), periarteriolar lymphatic sheath (PALS), GC, and marginal zone (MZ) (×400); F, RP with splenic cords (SC) and venous sinuses (VS) (hematoxylin and eosin, ×400); G, almost normal shape of thin, delicate elastic fibers in the lymph node (arrow) (Orcein, ×400); H, nearly normal shape of thin, elastic fibers (arrow) in the spleen (Orcein, ×400); I, almost normal mast cell size and numbers (arrows) in the pericapsular connective tissue of the lymph node (toluidine blue, ×400).

WP with thick dilated CA (Fig. 2E), RP with congested VS and dilated PA (Fig. 2F), irregular thick elastic fibers of LNs (Fig. 2G), thick elastic fiber aggregation in the spleen (Fig. 2H), and increased numbers and larger than normal mast cells in the pericapsular connective tissue of LNs (Fig. 2I).

Rats treated with *Moringa oleifera*, curcumin, GTE, and combined curcumin and GTE showed marked improvements in LN histoarchitecture without visible lesions (Figs. 3, 4, 5, 6A-C). These rats also showed large improvements in spleen histoarchitecture without marked lesions (Figs. 3, 4, 5, 6D-F), whilst the CP treatment group showed slight improvements in LN structure, but cortical changes appeared as lymphocytic loss in GCs due to degenerated cells (Fig. 7B), also showing slight improvements in spleen structure due to WP with a dilated CA (Fig. 7E). All those experimental groups showed marked improvements in area percentage and shape of elastic fibers in LNs (Figs. 3, 4, 5, 6, 7D) and spleen, as shown in Figures 3, 4, 5, 6 and 7G, H, and also showed

restoration of the normal number and shape of mast cells (Figs. 3, 4, 5, 6, 7I).

Morphometrical analysis

Table II shows significant increase in elastic fiber area in the LN (21.62 ± 2.15 %) and in red pulp spleen (18.77 ± 1.84 %) of the benzene-treated group when compared with their respective controls, and significant decrease in elastic fiber area in the groups treated with *Moringa oleifera*, curcumin, GTE, combined curcumin and GTE, and CP when compared to that in the leukemia positive control group. This shows great improvement in the mean area percent values in the treated groups. Table II also shows significant increase in mast cell counts (12.50 ± 3.44) in the MLN sections in the benzene-treated group compared to that of the control group (4.20 ± 1.03). There is also a significant decrease in the mast cell count in the groups treated with *Moringa oleifera*, curcumin, GTE, combined curcumin and GTE, and CP when compared to that in the leukemia-positive control group.

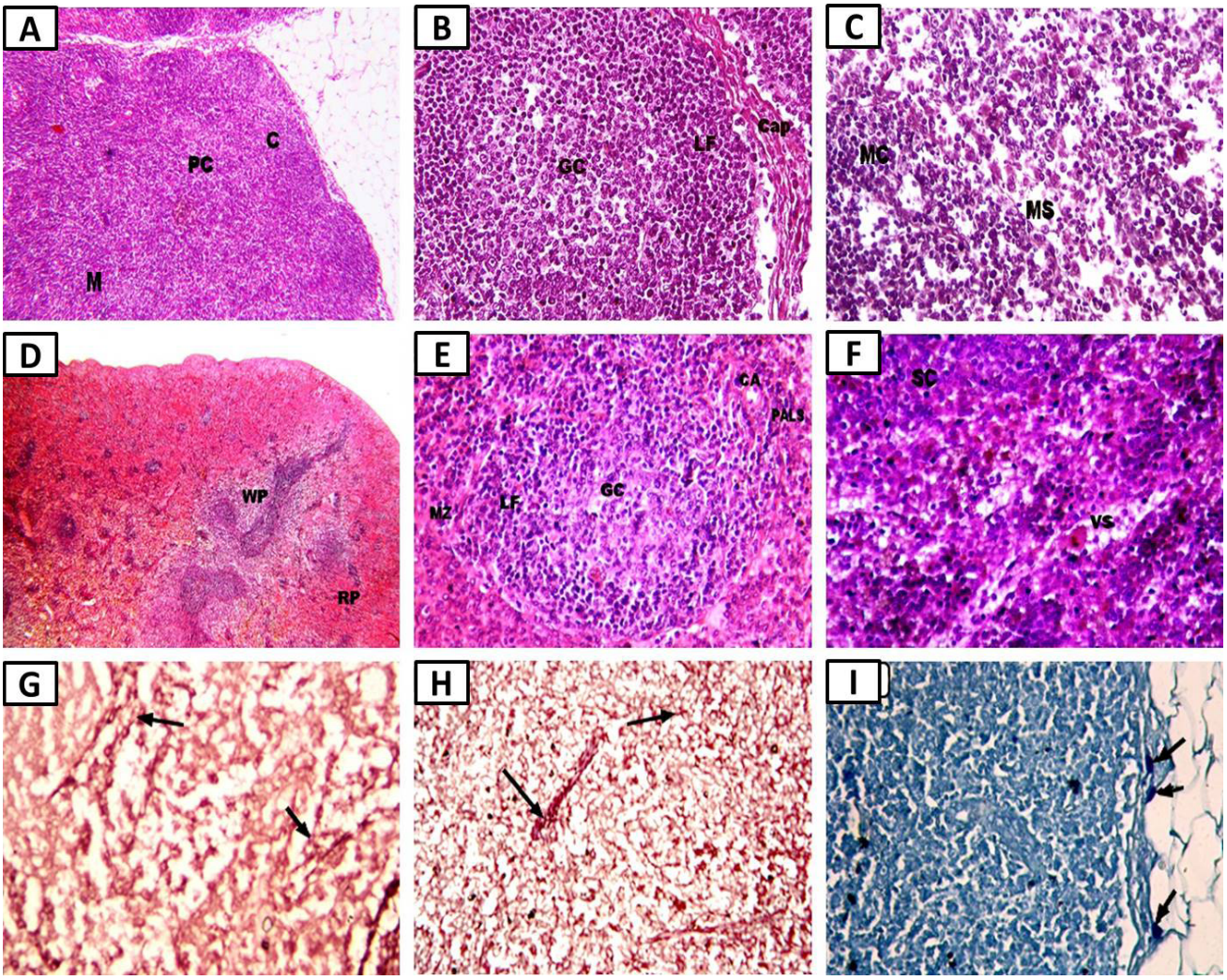

Fig. 4. Photomicrographs of the curcumin treatment group showing: A, marked improvement in lymph node structure with cortex (C), paracortex (PC), and medulla (M) (×100); B, cortical lymphoid follicle (LF) with germinal center (GC) (×400); C, medulla with medullary cords (MC) and medullary sinuses (MS) (×400); D, marked improvement in spleen white pulp (WP) and red pulp (RP) structure (×100); E, WP with LF, central arteriole (CA), periarteriolar lymphatic sheath (PALS), GC, and marginal zone (MZ) (×400); F, RP with splenic cords (SC) and venous sinuses (VS) (hematoxylin and eosin, ×400); G, almost normal shape of thin, delicate elastic fibers in the lymph node (arrow) (Orcein, ×400); H, nearly normal shape of thin, elastic fibers (arrow) in the spleen (Orcein, ×400); I, almost normal mast cell size and numbers (arrows) in the pericapsular connective tissue of the lymph node (toluidine blue, ×400).

Table II.- Mean ± SD for elastic fibers area percent (%) in lymph node and spleen and for mast cell count in lymph node of leukemia positive control against other treatment groups.

Group	Control (n=10)	Benzene treated (n=10)	MO treated (n=10)	Curcumin treated (n=10)	GTE treated (n=10)	GTE+ curcumin treated (n=10)	CP treated (n=10)
Elastic fiber area % of lymph node	9.95 ± 1.17	21.62 ± 2.15*	11.10 ± 2.20	11.90 ± 1.16	12.70 ± 0.62	10.66 ±1.15	10.59 ± 1.00
Elastic fiber area % of Spleen	9.70 ± 1.95	18.77 ± 1.84*	11.22 ± 1.24	11.69 ± 1.50	12.48 ± 1.54	11.12 ± 1.09	10.54 ± 1.45
Mast cell count of lymph node	4.20 ± 1.03	12.50 ± 3.44*	5.00 ± 2.16	5.40 ± 1.71	6.00 ± 1.41	4.80 ± 1.03	4.60 ± 1.35

MO, *Moringa oleifera*; GTE, green tea extract; CP, cyclophosphamide. *, significant difference between the leukemia positive control group (2) and other treatment groups ($p \leq 0.05$).

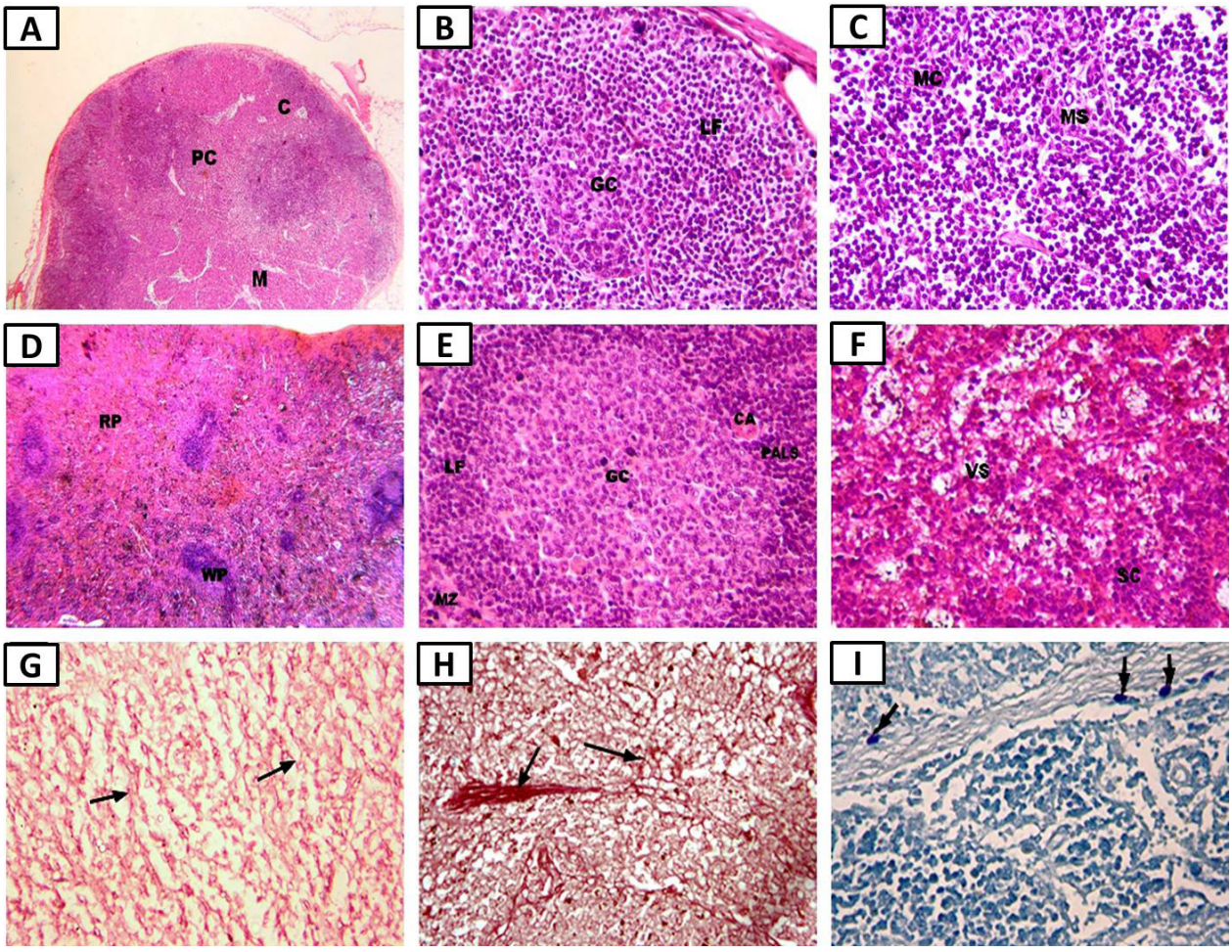

Fig. 5. Photomicrographs of the green tea treatment group showing: A, marked improvement in lymph node structure with cortex (C), paracortex (PC), and medulla (M) (×100); B, cortical lymphoid follicle (LF) with germinal center (GC) (×400); C, medulla with medullary cords (MC) and medullary sinuses (MS) (×400); D, marked improvement in spleen white pulp (WP) and red pulp (RP) structure (×100); E, WP with LF, central arteriole (CA), periarteriolar lymphatic sheath (PALS), GC, and marginal zone (MZ) (×400); F, RP with splenic cords (SC) and venous sinuses (VS) (hematoxylin and eosin, ×400); G, almost normal shape of thin, delicate elastic fibers in the lymph node (arrow) (Orcein, ×400); H, nearly normal shape of thin, elastic fibers (arrow) in the spleen (Orcein, ×400); I, almost normal mast cell size and numbers (arrows) in the pericapsular connective tissue of the lymph node (toluidine blue, ×400).

DISCUSSION

In this study, complete blood count and differential leukocyte count showed a significant increase in WBC counts (marked leukocytosis), decreased RBC count (anemia), decreased Hb concentration (hemoglobinemia), decreased PCV, and decreased Figurelet count in the benzene-treated group when compared to that of the control group. This demonstrates the successful induction of leukemia in rats by benzene injection, which is in line with a previous leukemia model of Olufemi*et al*. (2014), who reported that leukemia was induced as significantly elevated WBC (leukocyte) counts and anemia in the control group.

The mechanism of leukemia induction is explained by Li *et al*. (2019), in which multiple key molecular and cellular events may be involved in myeloid leukemogenesis. Exposure to environmental factors, including chemicals and ionizing radiation, is a risk factor for AML and myelodysplastic syndrome. After exposure, benzene undergoes metabolism by cytochrome P450 2E1 and 2F1, mainly in the liver. Benzene exerts its toxicity through reactive metabolites, that is, catechol, hydroquinone, benzoquinone, and others.

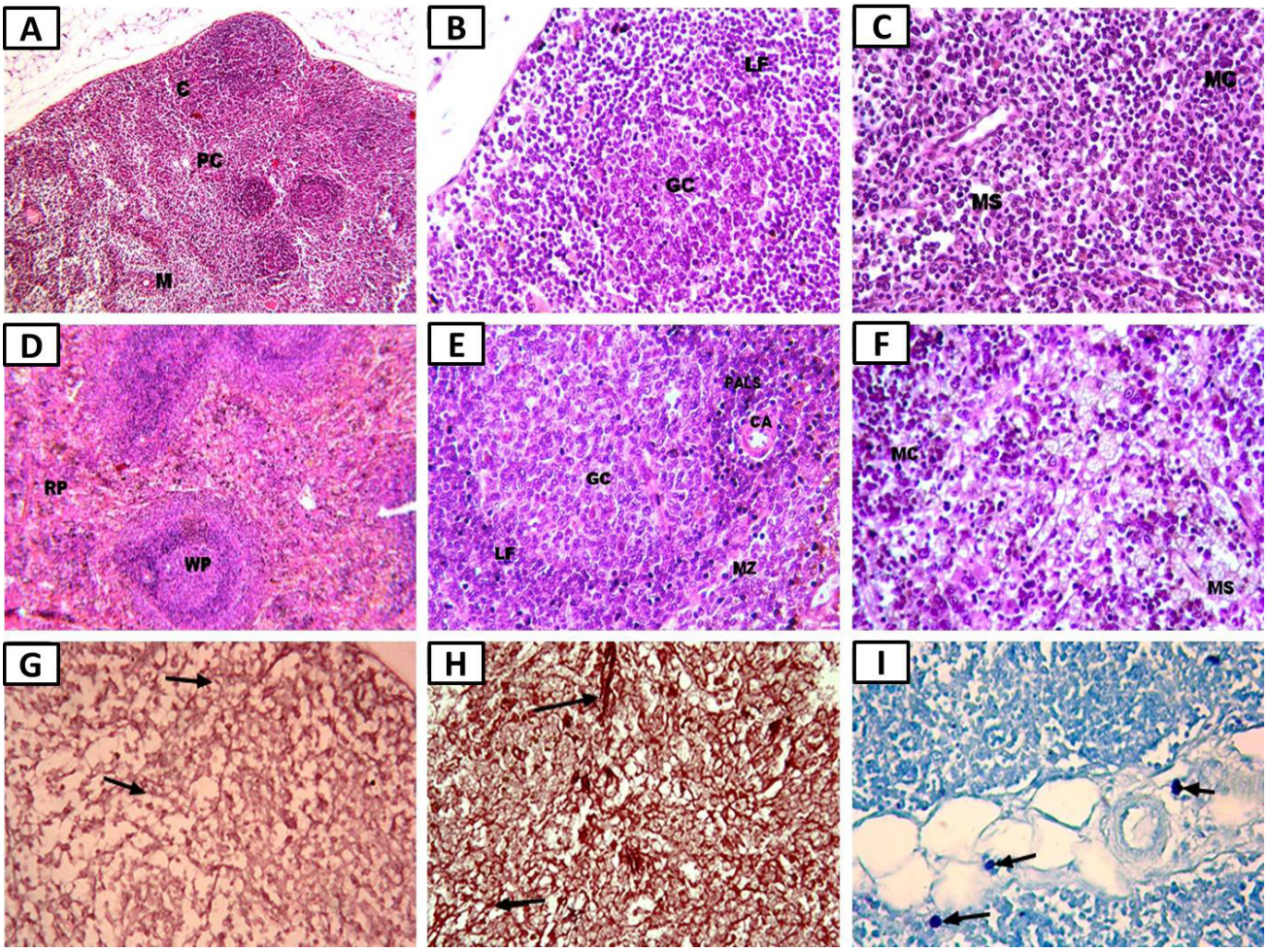

Fig. 6. Photomicrographs of the combined curcumin and green tea extract treatment group showing: A, obvious improvement in lymph node structure with cortex (C), paracortex (PC), and medulla (M) (×100); B, cortical lymphoid follicle (LF) with germinal center (GC) (×400); C, medulla with medullary cords (MC) and medullary sinuses (MS) (×400); D, obvious improvement in spleen white pulp (WP) and red pulp (RP) structure (×100); E, WP with LF, central arteriole (CA), periarteriolar lymphatic sheath (PALS), GC, and marginal zone (MZ) (×400); F, RP with splenic cords (SC) and venous sinuses (VS) (hematoxylin and eosin, ×400); G, almost normal shape of thin, delicate elastic fibers in the lymph node (arrow) (Orcein, ×400); H, nearly normal shape of thin, elastic fibers (arrow) in the spleen (Orcein, ×400); I, almost normal mast cell size and numbers (arrows) in the pericapsular connective tissue of the lymph node (toluidine blue, ×400).

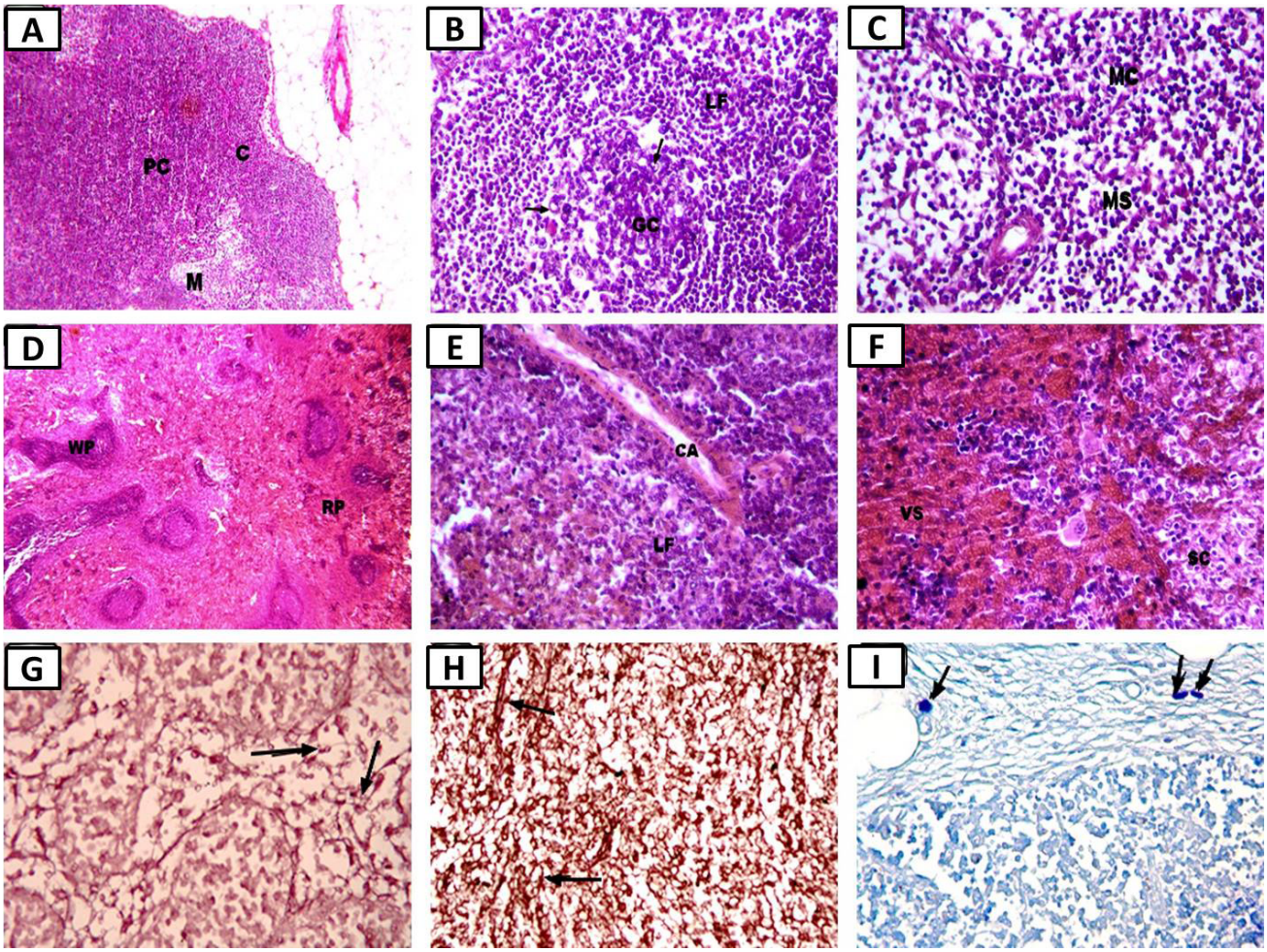

Fig. 7. Photomicrographs of the cyclophosphamide treatment group showing: A, slight improvement in the whole structure of the lymph node (×100); B, cortical changes with some lymphocytic depletion in germinal centers and some necrotic degenerated cells (ghost cell) (arrows) (×400); C, medulla with medullary cords (MC) and medullary sinuses (MS) (×400); D, slight improvement in spleen white pulp and red pulp structure (×100); E, white pulp with dilated central arteriole (CA) in non-active lymphoid follicle (LF) (×400); F, red pulp with dilated and congested venous sinuses (VS) and splenic cords (SC) (hematoxylin and eosin, ×400); G, almost normal shape of thin, delicate elastic fibers in the lymph node (arrow) (Orcein, ×400); H, nearly normal shape of thin, elastic fibers (arrow) in the spleen (Orcein, ×400); I, almost normal mast cell size and numbers (arrows) in the pericapsular connective tissue of the lymph node (toluidine blue, ×400).

Benzene and its metabolites redistribute and accumulate in bone marrow tissue, where they exert their selective toxicity to hematopoietic stem cells or progenitor cells (Khalade *et al*., 2010). The resultant molecular and cellular effects include oxidative stress, changes in gene expression and function, and a disrupted balance in proliferation, differentiation, apoptosis, and cytogenetic abnormalities, such as chromosomal aberrations (Maiti *et al*., 2019; Musial *et al*., 2020). Benzene metabolites interact with hematopoietic cells at different differentiation stages in bone marrow, resulting in genetic, chromosomal, or epigenetic abnormalities, genomic instability, and altered proliferation and differentiation of hematopoietic stem cells, leading to the formation of mutated hematopoietic cells and subsequent clonal evolution to leukemia (Roy *et al*., 2014).

The amelioration of blood parameters measured by treatment with *Moringa oleifera*, curcumin, and GTE revealed the anti-leukemic action of these herbs. The anti-leukemic action of *Moringa oleifera* is supported by Akanni *et al*. (2014), who reported the chemopreventive and anti-leukemic activities of ethanol extracts of *Moringa oleifera* leaves similar to the standard anti-leukemic drug. The *Moringa oleifera* ethanol extracts ameliorated induced

leukemic conditions in the affected rats owing to its bioactive constituents in benzene-induced leukemia rats. Additionally, the authors reported that the extract might be an active, natural, and non-toxic anticancer drug lead.

Hashim *et al*. (2012) has showed that curcumin has cytotoxic activity against leukemia cell lines and possesses anticancer activity by inhibiting cell growth activity, which show characteristic features of apoptosis. A population-based study by Kuo *et al*. (2009) has revealed that drinking large amounts of green tea containing more than 550 units of catechins decreases the risk of leukemia. EGCG also induced necrosis-like cell death in chronic myeloid leukemia cells, overcoming apoptosis resistance (Yao *et al*., 2017).

In the present study, Benzene Chromasolv caused a histological damages of the LNs and spleen, which also increased the percentage of non-organized thick elastic fibers in the LN and spleen, and elicited a strong inflammatory response represented by elevated mast cell counts in LN sections. These findings are in accordance with Akanni *et al*. (2014), who found that groups exposed to benzene carcinogen show varying lesions of the heart (mild to marked), coronary congestion, severe vacuolar degeneration and necrosis of hepatocytes with cellular infiltration by mononuclear cells, and diffuse tubular degeneration and necrosis with renal interstitial hemorrhage. Additionally, Hetal (2016) has found that liver tissues exhibit severe damage, such as sinusoidal dilation and necrosis due to benzene exposure. The various lesions in the LNs and spleen in this study are attributed to the DNA damaging ability of the agent (Nakajima *et al*., 2019).

Increased mast cells in the benzene group are explained by Sureshkumar *et al*. (2005), who concluded that the general pathological response to a toxicant triggers acute inflammatory immune processes. The authors reported that these changes were most probably due to the irritative effect of benzene, recruitment of inflammatory cells, and release of many inflammatory mediators, reactive oxygen species (ROS), or free radicals. A possible explanation for the ameliorative role of *Moringa oleifera*, curcumin, GTE, and combined curcumin and GTE treatment on the toxic effects of Benzene Chromasolv on LN and spleen structure could be the involvement of their antioxidant and scavenging properties. Antioxidants provide protection or remediation by scavenging ROS that damage DNA and initiate diseases, such as cancer (Aziz *et al*., 2019).

In the present study, CP treatment caused toxic changes in the LN and spleen structure, which was suggestive of the deleterious effects of CP on normal cells after prolonged usage. These findings are supported by Lee *et al*. (2010), who concluded that CP has severe and life-threatening adverse effects, including AML, bladder cancer, and permanent infertility, especially at higher doses. Thus, the aggravated damage to the organs of rats co-treated with CP and Benzene Chromasolv was suggestive of the deleterious effects of CP (anticancer drug) on normal cells after prolonged usage. The increased elastic fiber area percentage (elastosis) in the benzene-treated group is explained by Jimenez *et al*. (2006), who discussed the causes of solar elastosis as "thickening, degraded elastic fibers, and tangled shapes of elastic fibers lead to increased amounts of degraded elastic fibers" due to premature proteolytic degradation and impaired remodeling by extracellular matrix components.

The observed loss of physiologically relevant elastic fibers is also affected by the fact that fully differentiated (adult) dermal fibroblasts lose their ability to synthesize new elastin and thus cannot replace damaged elastic fibers (Roy *et al*., 2014). As elastic fibers are solely responsible for elasticity/resilience, there is an obvious need for the development of methods that might protect existing elastic fibers from premature degradation by elastolytic proteinases and facilitate new elastogenesis. Another possible mechanism is proposed by Philips *et al*. (2004), who reported that benzene and its derivatives increase the expression of elastin, synthesized primarily by fibroblasts. In the present study, *Moringa oleifera*, curcumin, and green tea treatment restored the normal elastic fiber formation/degradation machinery in both LNs and spleens, as represented by a decrease in the elevated elastic fiber area percent. This may be explained by the fact that polyphenols synergistically enhance elastogenesis induced by selected elastogenic compounds in dermal fibroblast cultures (Jimenez *et al*., 2006).

CONCLUSION

From the present study, it appears that *Moringa oleifera*, curcumin, GTE, and combined curcumin and GTE treatment could play an ameliorative and curative function against benzene-induced histological changes in the LN and spleen sections of leukemic rats.

ACKNOWLEDGEMENT

This work was supported by grants from the Taif University Researchers Supporting Program (project number: TURSP-2020/151), Taif University, Saudi Arabia.

Statement of conflict of interest

The authors declare that they have no known competing financial interests or personal relationships that could have appeared to influence the work reported in this paper.

REFERENCES

Abdellatef, E., Daffalla, H.M., Nassrallah, A.A., Aboul-Enein, K.M., El-Shemy, H.A. and Khalafalla, M.M., 2010. Antiproliferative action of *Moringa oleifera* Lam. root extracts in acute myeloid leukemia (AML) cell line. *J. exp. Sci.,* **1**: 27-28.

Ahmadi, Z., Shariati, A.A., Fayazi, S. and Latifi, M., 2016. The association between lifestyle and incidence of leukemia in adults in Ahvaz. *Iran. J. Chronic Dis. Care*, **5**: e59492. https://doi.org/10.17795/jjcdc-32924

Akanni, E.O., Adedeji, A.L., Akanni, R.A. and Oloke, J.K., 2014. Up-regulation of TNF-α by ethanol extract of *Moringa oleifera* in benzene-induced leukemic wister rat: A possible mechanism of anticancer property. *Cancer Res.,* **74**: 3792. https://doi.org/10.1158/1538-7445.AM2014-3792

Aziz, M.A., Diab, A.S. and Mohammed, A.A., 2019. Antioxidant categories and mode of action. In: *Antioxidants.* InTech Open. https://doi.org/10.5772/intechopen.83544

Chen, Y., Jia, Y., Song, W. and Zhang, L., 2018. Therapeutic potential of nitrogen mustard based Hybrid molecules. *Front. Pharmacol.*, **9**: 1453. https://doi.org/10.3389/fphar.2018.01453

Culling, C. and Albert, F., 2013. *Handbook of histopathological and histochemical techniques: Including museum techniques.* Butterworth-Heinemann Books, Oxford, United Kingdom.

Fares, M., 2015. In vitro *studies on anti-leukemic effects of tetracycline's analogues and cyclophosphamide.* INST för Laboratoriemedicin, Dept of Laboratory Medicine, R 64, Karolinska University Hospital, Huddinge.

Ghosh, S., Krieg, R.J., Sica, D.A., Wang, R., Fakhry, I. and Gehr, T., 2009. Cardiac hypertrophy in neonatal nephrectomized rats: The role of the sympathetic nervous system. *Pediat. Nephrol.,* **24**: 367-377. https://doi.org/10.1007/s00467-008-0978-8

Hashim, F.J., Shawkat, M.S. and Al-Jewari, H., 2012. Cytotoxicity of curcumin against leukemic cell lines via apoptosis activity. *Curr. Res. J. biol. Sci.*, **4**: 60-64.

Hetal, R., 2016. Evaluation of benzene induced histopathological alterations in the rat. *Int. J. Adv. Res.*, **4**: 563-567. https://doi.org/10.21474/IJAR01/685

Jimenez, F., Mitts, T.F., Liu, K., Wang, Y. and Hinek, A., 2006. Ellagic and tannic acids protect newly synthesized elastic fibers from premature enzymatic degradation in dermal fibroblast cultures. *J. Investig. Dermatol.*, **126**: 1272-1280. https://doi.org/10.1038/sj.jid.5700285

Ke, X. and Shen, L., 2017. Molecular targeted therapy of cancer: The progress and future prospect. *Front. Lab. Med.*, **1**: 69-75. https://doi.org/10.1016/j.flm.2017.06.001

Khalade, A., Jaakkola, M.S., Pukkala, E. and Jaakkola, J.J.K., 2010. Exposure to benzene at work and the risk of leukemia: a systematic review and meta-analysis. *Environ. Hlth.*, **9**: 1-8. https://doi.org/10.1186/1476-069X-9-31

Kumazoe, M., Tsukamoto, S., Lesnick, C., Kay, N.E., Yamada, K., Shanafelt, T.D. and Tachibana, H., 2015. Vardenafil, a clinically available phosphodiesterase inhibitor, potentiates the killing effect of EGCG on CLL cells. *Br. J. Haematol.*, **168**: 610-613. https://doi.org/10.1111/bjh.13135

Kuo, Y.C., Yu, C.L., Liu, C.Y., Wang, S.F., Pan, P.C., Wu, M.T., Ho, C.K., Lo, Y.S., Li, Y. and Christiani, D.C., 2009. A population-based, case–control study of green tea consumption and leukemia risk in southwestern Taiwan. *Cancer Causes Contr.*, **20**: 57-65. https://doi.org/10.1007/s10552-008-9217-7

Laurence, D.R. and Bacharach, A.L., 2013. *Evaluation of drug activities: Pharmacometrics.* Elsevier.

Lee, Y.C., Park, J.S., Lee, C.H., Bae, S.C., Kim, I.S., Kang, C.M. and Kim, G.H., 2010. Hyponatraemia induced by low-dose intravenous pulse cyclophosphamide. *Nephrol. Dialysis Transplant.*, **25**: 1520-1524. https://doi.org/10.1093/ndt/gfp657

Li, L., Cui, Y., Shen, J., Dobson, H. and Sun, G., 2019. Evidence for activated Lck protein tyrosine kinase as the driver of proliferation in acute myeloid leukemia cell, CTV-1. *Leukemia Res.*, **78**: 12-20. https://doi.org/10.1016/j.leukres.2019.01.006

Maiti, S., Nazmeen, A., Medda, N., Patra, R. and Ghosh, T.K., 2019. Flavonoids green tea against oxidant stress and inflammation with related human diseases. *Clin. Nutr. Exp.*, **24**: 1-14. https://doi.org/10.1016/j.yclnex.2018.12.004

Musial, C., Kuban-Jankowska, A. and Gorska-Ponikowska, M., 2020. Beneficial properties of green tea catechins. *Int. J. mol. Sci.*, **21**: 1744. https://doi.org/10.3390/ijms21051744

Nakajima, T., Vares, G., Ninomiya, Y., Wang, B., Katsube, T., Tanaka, T., Maruyama, K. and Nenoi, M., 2019. Diallyl disulfide mitigates DNA damage and spleen tissue effects after irradiation. *Int. med. J. exp. clin. Res.*, **25**: 8920-8927. https://doi.org/10.12659/MSM.917207

Netíková, I.R., Petruželka, L., Šťastný, M. and Štengl, V., 2018. Safe decontamination of cytostatics

from the nitrogen mustards family. Part one: Cyclophosphamide and ifosfamide. *Int. J. Nanomed.*, **13**: 7971. https://doi.org/10.2147/IJN.S159328

Olufemi, A.E., Folarin, O.R. and Igbeneghu, C., 2014. Tumour suppressive and organ protective effects of aqueous andrographis paniculata leaves extract on benzene induced leukaemia bearing rats. *Annu. Res. Rev. Biol.,* **4**: 1070-1079. https://doi.org/10.9734/ARRB/2014/6886

Philips, N., Burchill, D., O'Donoghue, D., Keller, T. and Gonzalez, S., 2004. Identification of benzene metabolites in dermal fibroblasts as nonphenolic: Regulation of cell viability, apoptosis, lipid peroxidation and expression of matrix metalloproteinase 1 and elastin by benzene metabolites. *Skin Pharmacol. Physiol.*, **17**: 147-152. https://doi.org/10.1159/000077242

Roy, S., Deb, N., Basu, S. and Besra, S.E., 2014. Apoptotic activity of ethanolic extract of *Moringa oleifera* root bark on human myeloid leukemia cells via activation of caspase cascade. *World J. Pharm. Sci.*, **3**: 1138-1156.

Sinha, D., Biswas, J., Sung, B., Aggarwal, B. and Bishayee, A., 2012. Chemopreventive and chemotherapeutic potential of curcumin in breast cancer. *Curr. Drug Targets*, **13**: 1799-1819. https://doi.org/10.2174/138945012804545632

Sureshkumar, V., Paul, B., Uthirappan, M., Pandey, R., Sahu, A.P., Lal, K., Prasad, A.K., Srivastava, S., Saxena, A. and Mathur, N., 2005. Proinflammatory and anti-inflammatory cytokine balance in gasoline exhaust induced pulmonary injury in mice. *Inhalation Toxicol.*, **17**: 161-168. https://doi.org/10.1080/08958370590904616

Tomita, M., Kawakami, H., Uchihara, J., Okudaira, T., Masuda, M., Takasu, N., Matsuda, T., Ohta, T., Tanaka, Y. and Ohshiro, K., 2006. Retracted: Curcumin (diferuloylmethane) inhibits constitutive active NF-κB, leading to suppression of cell growth of human T-cell leukemia virus type I-infected T-cell lines and primary adult T-cell leukemia cells. *Int. J. Cancer*, **118**: 765-772. https://doi.org/10.1002/ijc.21389

Varkesh, H., Mokhtari, N., Moeini, M., Baser, R.S., Masoomi, Y. and Moeini, M., 2013. The dentist's role in improving the life's quality of children with leukemia. *Am. J. Res. Commun.*, **1**: 66-7.

Verma, R.K., Kumari, P., Maurya, R.K., Kumar, V., Verma, R.B. and Singh, R.K., 2018. Medicinal properties of turmeric (*Curcuma longa* L.): A review. *Int. J. chem. Stud.*, **6**: 1354-1357.

Yao, S., Zhong, L., Chen, M., Zhao, Y., Li, L., Liu, L., Xu, T., Xiao, C., Gan, L. and Shan, Z., 2017. Epigallocatechin-3-gallate promotes all-trans retinoic acid-induced maturation of acute promyelocytic leukemia cells via PTEN. *Int. J. Oncol.*, **51**: 899-906. https://doi.org/10.3892/ijo.2017.4086